318 Riggs Hall
Clemson, South Carolina P-32
29634-0921

Mechanical Engineering Department
College of Engineering
Clemson University
Clemson, South Carolina

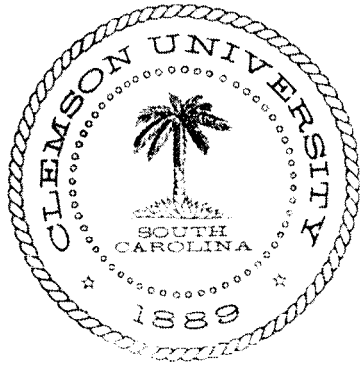

FINAL REPORT NASA GRANT NSG-1297

FRACTURE AND CRACK GROWTH IN ORTHOTROPIC LAMINATES

December 1, 1985

Principal Investigator

James G. Goree
Professor of Mechanics and
Mechanical Engineering

Graduate Assistant

Autar K. Kaw
Ph.D. Candidate in Engineering Mechanics

Department of Mechanical Engineering
College of Engineering
Clemson University
Clemson, South Carolina 29634

ABSTRACT

A mathematical model based on the classical shear-lag assumptions is used to study the residual strength and fracture behavior of composite laminates with symmetrically placed buffer-strips. The laminate is loaded by a uniform remote longitudinal tensile strain and has initial damage in the form of a transverse crack in the parent laminate between buffer-strips. The crack growth behavior as a function of material properties, number of buffer-strip plies, spacing, width of buffer-strips, longitudinal matrix splitting, and debonding at the interface is studied.

Buffer-strip laminates are shown to arrest fracture and increase the residual strengths significantly over those of one material laminates, with S-glass being a more effective buffer strip material than Kevlar in increasing the damage tolerance of Graphite/epoxy panels. For a typical Graphite/epoxy laminate with S-glass buffer-strips, the residual strength is about 2.4 times the residual strength of an all Graphite/epoxy panel with the same crack length. Approximately, 50% of this increase is due to the S-glass/epoxy buffer-strips, 40% due to longitudinal splitting of the buffer strip interface and 10% due to debonding. The optimum aspect ratio of spacing-to-width of buffer-strips is shown to be about four to one. Predicted remote failure strains are found to agree reasonably well with independently published experimental results.

ACKNOWLEDGEMENT

The principal investigator wishes to express his sincere appreciation to the Fatigue and Fracture Branch of the National Aeronautics and Space Administration for the support of this investigation under NASA Grant NSG-1297. In particular, the continued support, guidance, and assistance of the grant monitor, Mr. C. C. Poe, Jr. is acknowledged.

TABLE OF CONTENTS

LIST OF FIGURES

CHAPTER I

INTRODUCTION

Over the years engineers have faced the challenge of designing advanced composite components to meet both structural and damage tolerant requirements. The use of buffer-strip, hybrid composites has been clearly demonstrated [1-5] to be a step forward in that direction. A typical buffer-strip laminate is shown in Figure 1, and is constructed by inserting at specific intervals, narrow parallel composite strips of appropriate physical and geometrical properties. Buffer-strips have been shown to arrest fracture and give extra load carrying capacity to a damaged laminate. The stiffness, weight, and strength of the undamaged laminate are not significantly affected by this replacement, but in a damaged laminate the residual strength can be considerably increased.

Previous work [6-10] at Clemson University has concerned the development of simple mathematical models which contain the important physical and geometrical properties of the composite and accurately represent the fundamental fracture behavior of a laminate. The first such model for a buffer strip laminate was developed by Goree and Dharani [9]. The intent was to be able to estimate the ultimate strain required to fail the hybrid unidirectional laminate shown in Figure 2, as well as to assist in understanding the crack growth characteristics. The same model was extended in [10] to include longitudinal matrix splitting at the interface of the buffer strip and the main panel.

Poe and Kennedy [5] conducted experiments to relate the strength of damaged panels to the buffer strip material and the layup of the basic laminate. Graphite/epoxy, which has proven its potential to reduce the weight and cost of aircraft structures, was the parent laminate used in the

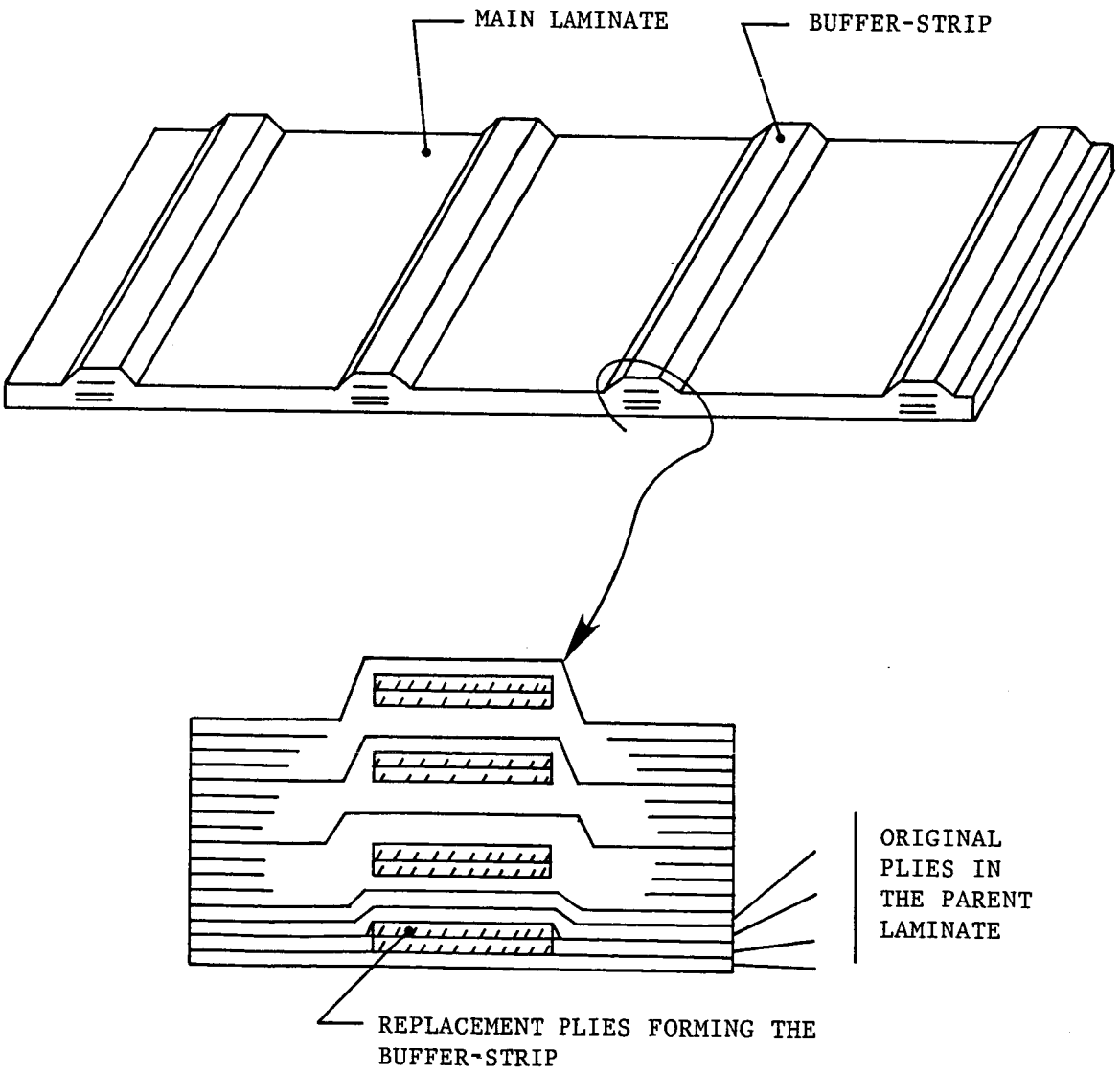

Figure 1. A Typical Buffer Strip-Laminate Configuration.

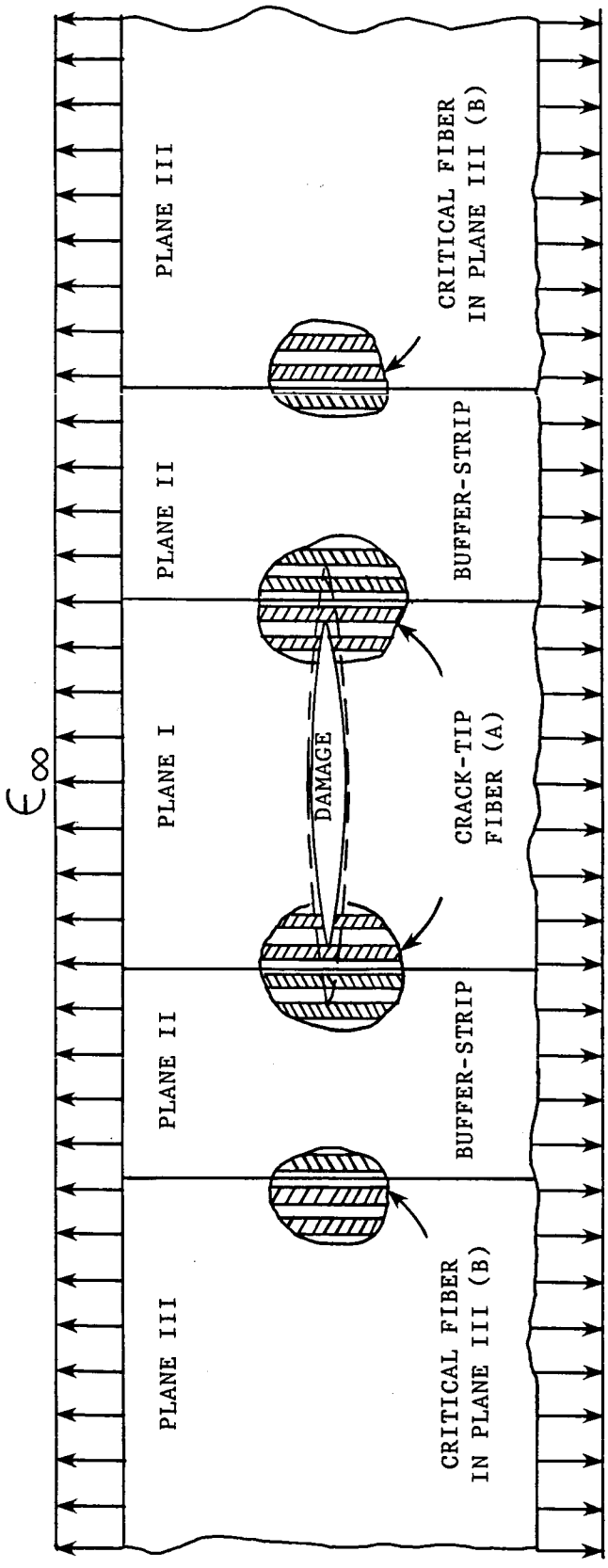

Figure 2. Geometry of a Symmetric Buffer-Strip Laminate.

above experimental investigation. Each panel was notched at the center between buffer-strips to represent initial damage. The panels were placed under tension and measurements of crack opening displacement, strains, and fracture behavior were taken. Two different laminates were used, $[45/0/-45/90]_{2S}$ and $[45/0/-45/0]_{2S}$, along with three different buffer-strip materials - S-glass/epoxy, Kevlar/epoxy and Mylar/epoxy; buffer-strip width and spacing were also varied. Buffer-strips were made by replacing only zero degree Graphite/epoxy plies by zero degree buffer material on a one-for-one or two-for-one replacement. A major emphasis of this report will be to compare the predicted behavior with that observed in [5].

In order to understand the development of the analysis developed during this study, it is important to point out the assumptions and the significant features of the model. The laminate is modeled as a two-dimensional region containing only unidirectional fibers as detailed in [10]. A typical laminate contains angle plies as well as zero degree plies, and these are accounted for by having constraining shear forces acting on the lateral surface of the zero degree lamina. The fibers are assumed to be linearly elastic and the matrix elastic-perfectly plastic. The fibers are considered to be of much higher strength and extensional stiffness than the matrix and all the axial load is assumed to be carried by the fibers. The matrix transfers the load by shear as given by the shear-lag assumptions [11-14]. By virtue of these assumptions the transverse and axial equilibrium equations are uncoupled. Therefore only the equilibrium equations in the longitudinal direction need be considered. Boundary conditions of a stress-free crack, uniform longitudinal remote strain, and symmetry about the center-line are enforced along with the equality of shear stresses on each of the adjacent regions at their respective interfaces. This results in a set of coupled

integral equations with unknown displacement and stress function integrands, [6-10].

A computer code, using Gauss and Laguerre quadrature rules was developed to solve for these unknown functions, [6-10]. The input and output parameters of the code are explained in the next section.

The objective of this report is not to discuss the formulation of the problem and the development of the solution technique, but to present in detail the fracture growth characteristics and remote failure strains as a function of initial damage, buffer-strip width and spacing, material properties, longitudinal matrix splitting, and debonding. These results are compared with the experimental results obtained by Poe and Kennedy [5]. The reader is referred to [6-10] for the mathematical formulation and solution techniques used to solve the related problems.

CHAPTER II

INPUT-OUTPUT PARAMETERS OF COMPUTER CODE

A computer code was prepared for the approximate shear-lag model using the Clemson University IBM 3081 digital computer, with the solution for a typical geometry taking about 28 minutes of computational time. On solving several test cases it was observed that the buffer-strip material and longitudinal splitting contributed by far the largest amount of the increase in remote failure strains as compared to the influence of debonding. This behavior is discussed in Chapter III. Excluding debonding from the solution for the combined case of buffer-strips and splitting decreased the number of integral equations by almost one-half. Since the computational time was proportional to the square of the number of integral equations, this reduced the computation time to about seven minutes.

INPUT PARAMETERS (Figure 3):

Half-width of main panel in number of equivalent fibers (NM)
Width of buffer-strip in number of equivalent fibers (NB)
Number of broken fibers in main panel (NBFI)
Number of broken fibers in buffer-strip (NBFII)
Ratio of stiffness of main panel to buffer strip (R)
Normalized split length at interface (α)

The geometric input parameters (NM,NB,NBFI,NBFII) of the model are given in terms of number of equivalent fiber bundles, whereas the experimental data is given in dimensions of length. To correlate the two the remote failing strain as a function of crack length for an all-Graphite/epoxy laminate [5] is compared to the Hedgepeth solution where remote failure strain is a function of the number of broken fibers for a unidirectional laminate (Table 1). That is, the Hedgepeth solution for a notched unidirectional

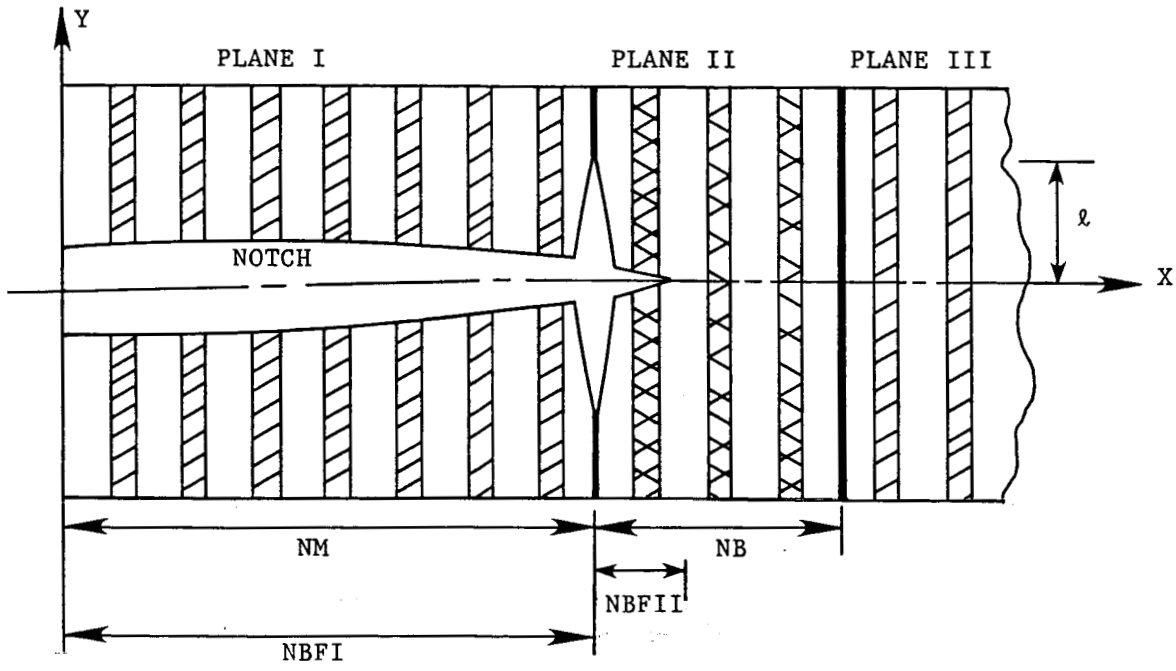

Figure 3. Input Parameters of the Computer Code.

Table 1. Correlation of analytical and experimental failure strains to obtain equivalent fiber spacing.

Hedgepeth Solution		Experimental Results	
Number of Broken Fibers	Failing Strain (%)	Crack Length (mms)	Failing Strain (%)
0	1.00	0	1.00
4	0.49	10	0.52
8	0.37	20	0.38
12	0.31	30	0.32
16	0.27	40	0.28

laminate with no splitting or yielding is required to match the observed failure of an all Graphite/epoxy laminate. Failure of the Hedgepeth model is assumed to occur when the first unbroken equivalent fiber bundle breaks. In the actual laminate failure is an abrupt self-similar brittle fracture as the presence of the off-axis plies significantly reduces the amount of crack-tip splitting and debonding. The hybrid buffer strip laminates, in comparison, have a large amount of both longitudinal splitting at the material interface as well as debonding between plies. This above procedure then gives a consistent way to relate the unidirectional model with the general laminate. The mathematical model for the buffer-strip material with crack-tip damage and the actual buffer-strip laminate are then compared using this equivalent fiber spacing. Using this method for a $[45/0/-45/0]_{2S}$ Graphite/epoxy laminate, an equivalent fiber bundle spacing of 2.6mms is required by the Hedgepeth model. For example, the test specimen in [5], represented in Table 1 had 13mms wide buffer-strip placed 51mms apart. This is represented in the model by buffer-strips of five fiber-spacings wide with twenty fiber-spacings between the strips. Note that the actual graphite fiber bundles in a fifty percent volume fraction laminate are on the order of 0.140mms apart. Requiring that the Hedgepeth model predict the behavior of

the above laminate groups about 20 graphite fiber bundles into one equivalent fiber.

The ratio of the stiffness of the main panel to that of the buffer-strip is denoted by R and is defined as

$$R = \sqrt{\frac{E_F^I}{E_F^{II}}} \quad , \tag{1}$$

where E_F^i = Young's modulus of the fiber in plane i,

i = I, II.

Note that the above ratio is obtained by assuming equal area of fibers, equal volume fraction, uniform laminate thickness and matrix composition throughout the composite. To account for the two-for-one replacement, where there are twice as many plies of the buffer material as the parent laminate, the Young's modulus and the ultimate failing stress of the buffer strip is taken to be double that of a single buffer strip. This assumption does not affect the ultimate failing strain of the buffer strip.

The normalized split length (α) is related to the actual split length 'ℓ' (Figure 3) by

$$\alpha = \sqrt{\frac{(G_M/h)t}{E_F A_F}}\ \ell \quad , \tag{2}$$

where G_M/h = equivalent shear stiffness modulus (N/m^3),

t = thickness of one unidirectional ply (m),

E_F = Young's modulus of the fiber (N/m^2), and

A_F = Cross-sectional area of one fiber (m^2).

All the above properties are for the parent laminate. The only unknown factor is (G_M/h) which, as explained in [6], is to be determined

experimentally. (G_M/h) accounts for the interaction between fibers [6,12,13]. 'G_M' and 'h' are typically not the matrix shear modulus and fiber bundle center-line spacings. They are assumed to be material constants and depend only on fiber and matrix properties, fiber volume fraction, orientation of plies, and not on the size of the damage region. Typical values of (G_M/h) found for Graphite/epoxy in [14] can be used to predict the order of magnitude of 'α' for typical split lengths. For example, from [14],

$G_M/h = 7.347 \times 10^{12}$ N/m^3,

t = 0.140 mms,

E = 285000 MPA, and

$A = 1.50 \times 10^{-8}$ m^2.

Equation (2) then gives

$\alpha = 1.6$ for ℓ=6 mms.

Note that A_F is the cross-sectional area of one fiber in the actual laminate as 'G_M/h' value is based on the actual laminate geometric and material properties.

OUTPUT PARAMETERS

Maximum stress concentration in plane I (KI)
Maximum stress concentration in plane II (KII)
Maximum stress concentration in plane III (KIII)

The remote failure strain (ε_∞) required to break a fiber in a plane is given by

$$\varepsilon_\infty = \frac{\varepsilon^i_{ult}}{K_i} \quad \text{, where} \tag{3}$$

ε^i_{ult} = ultimate failure strain of the fiber in plane i, and

K_i = maximum stress concentration in plane i.

The stability of crack growth in a particular laminate depends on the remote strain required to break fibers at the crack-tip as well as the remote strain required to fail the laminate catastrophically. This concept will be exemplified in the following sections. For the discussion of the results, the remote failure strains (ε_∞) is normalized with respect to the ultimate failure strain of an unnotched all Graphite/epoxy laminate.

CHAPTER III

RESULTS

The following discussion is divided into four parts with the influence of buffer-strips without interface splitting and debonding presented first. Next, the effects of longitudinal splitting is added to the buffer-strip results, and finally debonding is considered. A detailed comparison is then made between the present analysis and the experimental results of Poe and Kennedy [5].

BUFFER-STRIP LAMINATES WITH NO LONGITUDINAL MATRIX SPLITTING:

Goree and Dharani discussed the results for the above case in [9] for a 30 fiber spacing between buffer-strips. As mentioned earlier, 20 fiber spacings between buffer-strips and 5 fiber spacing wide buffer-strips is equivalent to the panels discussed in [5]. Figure 4 shows results for an initial crack growth in plane I, crack arrest at the interface, crack growth in the buffer-strip and subsequent failure of the laminate (9). Graphite/epoxy panels with S-glass/epoxy and Kevlar/epoxy buffer-strips are considered. The solid line is the normalized remote failure strain required to break the first fiber in front of the notch (fiber A) while the dotted line is the normalized remote strain required to break the first fiber in plane III (fiber B). Results for an all Graphite/epoxy laminate are also given. The crack grows by breaking consecutive fibers from the crack-tip to the interface. On reaching the interface the crack is arrested, as a larger remote strain is required to continue growth beyond the interface. As the crack grows into the buffer-strip the strain required to break the crack-tip fiber continues to increase, that is, the crack growth is stable. On the other hand, the strain required to break the first fiber in plane III

	E_F (MPA)	σ_{ult} (MPA)	ϵ_{ult} (PERCENT)
GRAPHITE	285000	2800	0.98
S-GLASS	100000	2800	2.30
KEVLAR	125000	2000	1.60

*ϵ_{ult} = ultimate failure strain of an all graphite/epoxy unnotched laminate.

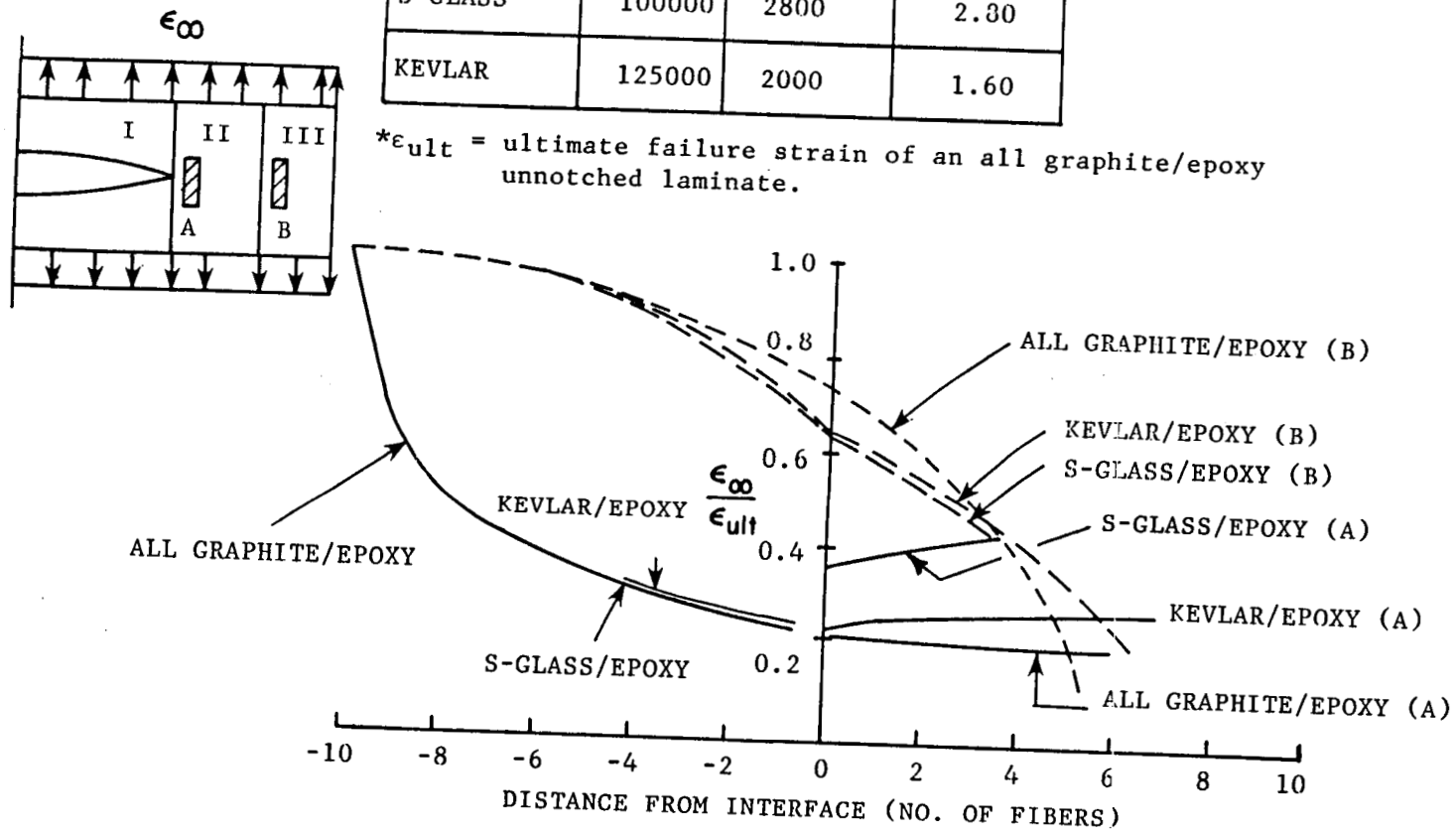

Figure 4. Normalized Remote Failure Strain as a Function of Crack Length.

decreases as the crack grows. When these two curves cross each other the laminate fails catastrophically.

The remote failure strains for S-glass/epoxy and Kevlar/epoxy buffer-strip laminates are 0.424 and 0.264 times the ultimate failure strain of the unnotched all Graphite/epoxy laminate, respectively.

In the case of S-glass/epoxy, all fibers in the buffer-strip do not break before failure of the first fiber in plane III, that is, the crack jumps the buffer-strip. On the contrary, all the fibers break in the Kevlar/epoxy buffer-strip before the first fiber in plane III fails. This is the result of a lower ultimate strain of Kevlar (1.60%) as compared to that of S-glass (2.80%).

Figure 5 demonstrates the effect of buffer-strip width on crack growth for a fixed spacing of 20 equivalent fibers between buffer-strips. The ultimate failure strain is plotted as a function of buffer-strip width for S-glass/epoxy. Similar to figure 3, the dotted line is the normalized remote strain required to break the first fiber in plane III (fiber B) and the solid line is the normalized remote failure strain required to break the first fiber in front of the notch (fiber A).

Figure 6 gives the optimum buffer-strip width for S-glass/epoxy and Kevlar/epoxy for a twenty fiber-spacing wide panel. The width is about 3-5 "fibers" for S-glass/epoxy and 3 "fibers" for Kevlar/epoxy. Similar results in [9] showed that the optimum aspect ratio for S-glass/epoxy should be four to one.

Figure 7 shows the remote failure strains for a two-for-one buffer-strip replacement as a function of crack length, other parameters remaining the same as in Figure 4. The crack growth in all of these laminates is no longer

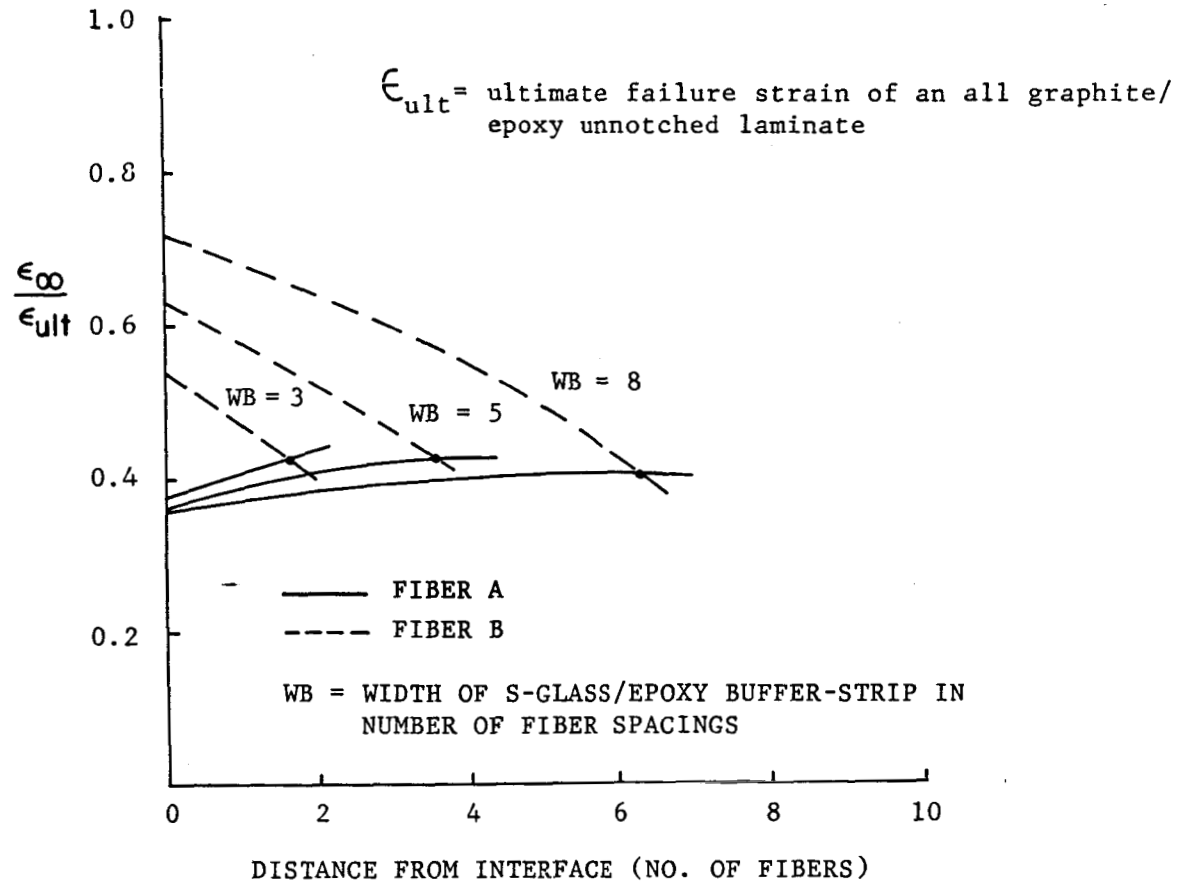

Figure 5. Normalized Remote Strain for Crack Growth as a Function of Buffer-Strip Width and Crack Length.

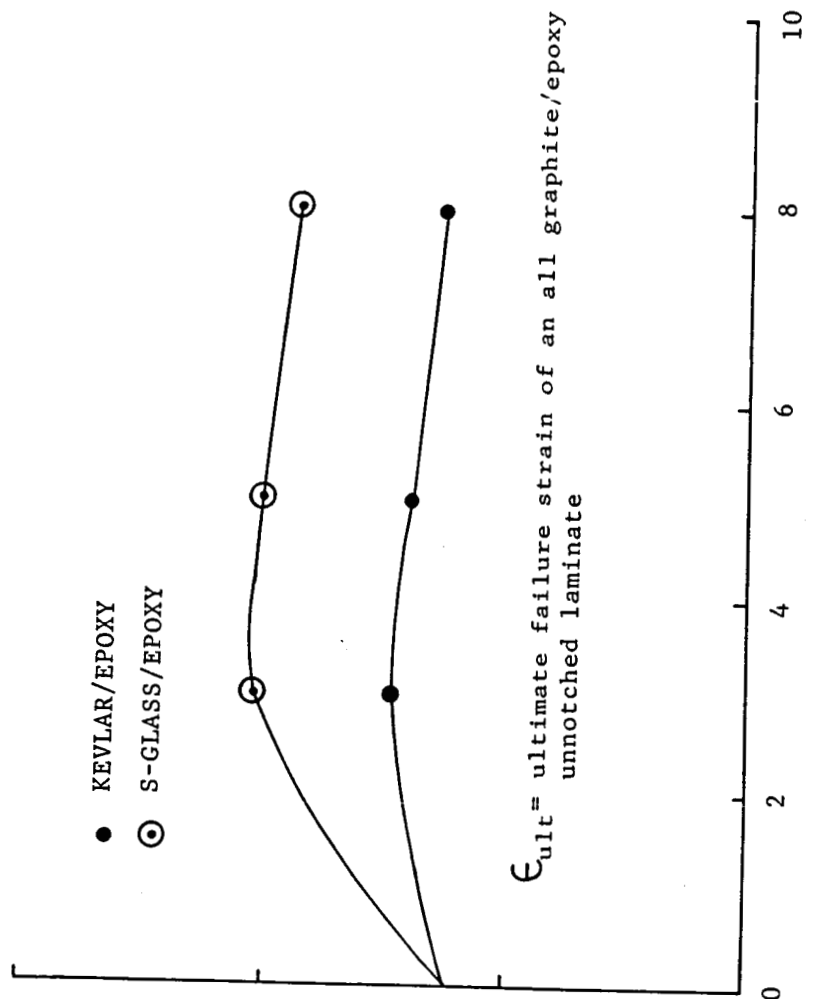

Figure 6. Normalized Remote Failure Strain as a Function of Buffer-Strip Width.

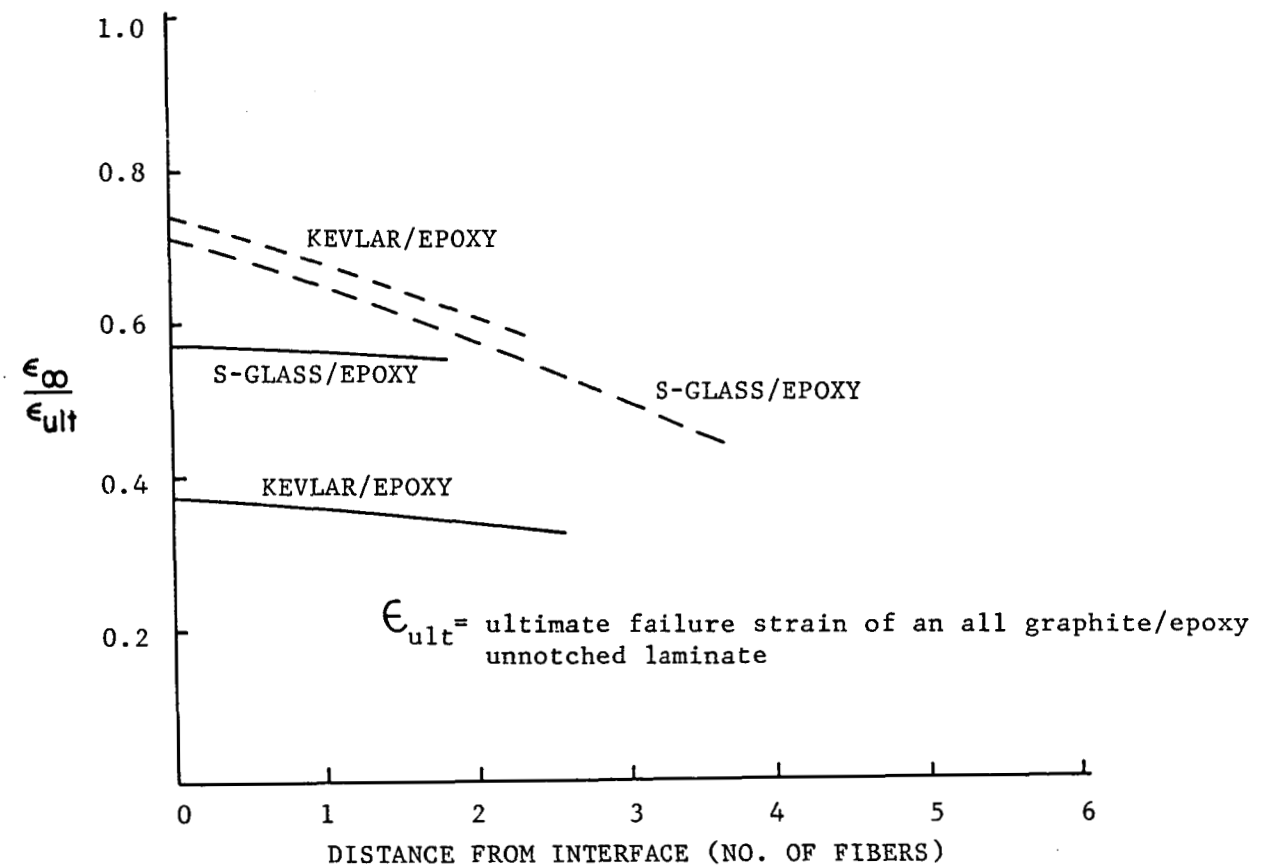

Figure 7. Normalized Remote Strain for Crack Growth as a Function of Crack Length for Two-for-One Replacement.

stable once it crosses the interface. The remote failure strains however, increase considerably over the one-for-one replacement as shown in Table 2.

Table 2. Effect of buffer-strip replacement thickness on normalized failure strains.

Buffer Strip	Normalized Remote Failure Strain	
	One-for-one replacement	Two-for-one replacement
Graphite/epoxy	0.245	0.358
S-glass/epoxy	0.424	0.570
Kevlar/epoxy	0.264	0.372

BUFFER-STRIP LAMINATES WITH LONGITUDINAL MATRIX SPLITTING:

Similar to Figure 4, Table 3 gives the normalized remote failure strain as a function of crack length for a typical normalized split length of 1.6 at the interface. The geometrical and physical parameters are the same as for Figure 4. The crack growth is arrested more effectively as compared to the no-split case. The crack jumps the S-glass/epoxy buffer-strip fully and an unstable growth follows. For the case of Kevlar/epoxy, the crack does not jump the buffer-strip but has an unstable crack growth once it breaks the crack-tip fiber. In the experimental investigation of [5] the same observations were made, where S-glass buffer-strips delaminated and pulled out from the Graphite/epoxy for most of the panel length, whereas the Kevlar buffer-strips were broken off at the fracture line.

Table 3. Normalized remote failure strain as a function of crack length.

No. of broken fibers in buffer-strip	Normalized remote strain required to fail	
	Crack-tip fiber	First fiber in Plane III
S-glass/epoxy		
0	0.609	0.571
1	0.595	0.556
Kevlar/epoxy		
0	0.384	0.600
1	0.360	0.579

Table 4 shows the effects of the S-glass/epoxy buffer-strip width on the remote failure strains of the laminate. The split length is kept constant for all cases. In Table 2, it was noticed that the crack jumps the S-glass/epoxy buffer-strip. If the buffer-strip width is increased however, the first fiber break will occur in the buffer-strip rather than in plane III. The minimum width required for this to occur is six fiber spacings. The crack growth still remains unstable.

Table 4. Normalized remote failure strain as a function of buffer-strip width.

Buffer-strip width	Normalized remote failure strain
4	0.534
5	0.571
6	0.603
7	0.598
8	0.594

From Table 4, it appears that six fiber spacings is the optimum width. Note that in the above analysis a constant split-length was used. A sensitivity analysis was carried out to investigate the effects of the length

of the split at the interface on the normalized remote failure strain. These results are shown in Figure 8 for the case of twenty fibers between the buffer-strips and five fiber-spacings wide buffer-strips. After a reasonable length of split occurs the remote failure strain becomes nearly constant with an increase in split length. A rapid increase is observed only during early split growth. Therefore, it appears reasonable to conclude that the results based on a constant split length of $\alpha = 1.6$ give a good measure of the laminate behavior.

EFFECTS OF DEBONDING:

Debonding in a buffer strip laminate for the case where splitting is not present gives a maximum increase in the remote failure strain of 8-12%. This maximum increase occurs for a debonding width of two-to-three fiber spacings and is independent of the initial crack length. The same behavior was found for an all Graphite/epoxy laminate in [8].

The computational time required to determine the remote failure strain increases four-fold for the case where debonding as well as splitting is considered. Also, the storage space required to run the program is out-of-limits for the IBM 3081 computer. Hence, a predicted remote failure strain for such cases is calculated on the basis of the results of the case where splitting is not present.

COMPARISON OF PREDICTED AND EXPERIMENTAL RESULTS:

An attempt is made to predict the remote failure strains for the laminates tested in [5]. Using the equivalent fiber spacing of 2.6mms and the geometrical and physical properties of the laminate of reference [14] in the model, the following results are obtained.

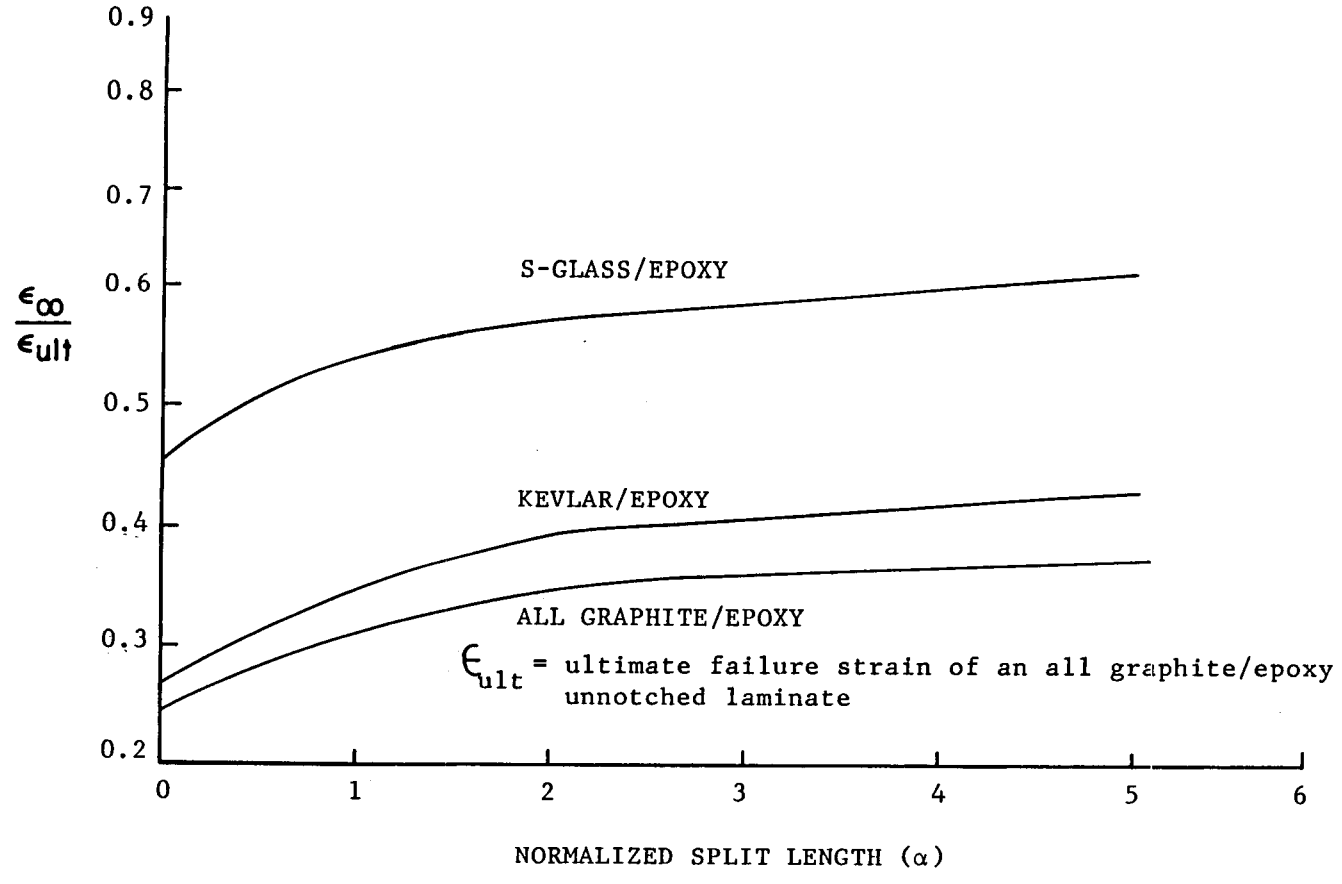

Figure 8. Normalized Remote Failure Strain as a Function of Normalized Split Length.

Table 5. Experimental and Analytical Remote Failure Strains of Buffer-Strip Panels with Arrested Fractures

Buffer Material	t_b/t_a	W_a	W_b	Normalized remote failure strain	
				Experimental	Predicted
S-glass/epoxy	1	51	13	0.581	0.571
	2	51	13	0.655	0.652
Kevlar/epoxy	1	51	13	0.389	0.384
	2	51	13	0.540	0.516

t_b/t_a = ratio of thickness of buffer-strip to the replaced Graphite/epoxy plies,

W_a = arrested crack length (mms),

W_b = width of buffer strip (mms).

Results are given next to indicate the effects of buffer-strip material, splitting, and debonding for the typical case of a 13mm wide S-glass/epoxy buffer-strips (one-for-one replacement) placed 51mms apart, as compared to an all Graphite/epoxy laminate.

EXPERIMENTAL RESULTS TAKEN FROM [5]

Net section (unnotched) of Gr/ep. without buffer-strips, $\frac{\varepsilon_\infty}{\varepsilon_{ult}} = 1.00$

51mms crack in Gr/ep. without buffer-strips, $\frac{\varepsilon_\infty}{\varepsilon_{ult}} = 0.244$

51mms crack in Gr/ep. with buffer-strips, $\frac{\varepsilon_\infty}{\varepsilon_{ult}} = 0.580$

ANALYTICAL RESULTS

Net section (unnotched) of Gr/ep. without buffer-strips, $\frac{\varepsilon_\infty}{\varepsilon_{ult}} = 1.00$

The results are given in Table 6 for the combinations of debonding and splitting.

Table 6. Analytical results for normalized remote failure strains for different combinations of debonding and splitting in a buffer-strip laminate.

NO BUFFER-STRIP:

Debonding	Splitting	Normalized remote failure strain
NO	NO	0.245
NO	YES	0.332
YES	NO	0.270

WITH BUFFER-STRIP:

Debonding	Splitting	Normalized remote failure strain
NO	NO	0.424
NO	YES	0.571
YES*	YES	0.585

The inclusion of the buffer-strip alone then increases the normalized failing strain from 0.245 to 0.424. Splitting at the interface gives a further increase to 0.571 and adding debonding gives a predicted normalized failure strain of 0.585. This gives a total increase of 0.340 (0.585-0.245) in the normalized remote failing strain. Of this increase, 53% is due to the

*The influence of debonding was approximated, based on the results of no splitting as previously discussed.

inclusion of buffer-strips, 43% due to longitudinal splitting and 4% due to debonding. While these results are for a particular laminate, it appears that the general trend of relative importance of the different controlling mechanisms is valid.

CHAPTER IV

CONCLUSIONS

A shear-lag model was used to study the effects of buffer-strip material, number of buffer-strip plies, spacing and width of buffer-strips, longitudinal matrix splitting, and debonding at the interface, on the remote failure strains and fracture growth characteristics of composite laminates. The results were compared with the experimental investigation [5] where Graphite/epoxy laminates with buffer-strips parallel to the loading direction were tested under uniform tensile strain in the presence of an initial transverse crack. The following were the significant results of the study:

(1) Buffer-strips arrested fracture except when the initial crack was small and the corresponding crack initiation loads were high. In general the residual strength increased significantly when the buffer-strip panels were used to arrest fracture.

(2) For a crack length of twenty fibers, the residual strength after crack arrest in a Graphite/epoxy laminate with S-glass buffer-strips was about 2.4 times the residual strength of an all Graphite/epoxy laminate with the same initial crack length.

(3) The optimum aspect ratio for S-glass/epoxy buffer-strips was about 4:1.

(4) S-glass buffer-strips contributed more than 50% of the increase in the remote failure strain.

(5) Splitting at the interface accounted for about 40% of the increase in the remote failure strain.

(6) Debonding typically represented less than 10% of the increase in the remote failure strain.

(7) The remote failing strain was not very sensitive to the longitudinal matrix split length.

(8) A two-for-one S-glass/epoxy buffer strip replacement gave an additional increase in the remote failing strain of about 20%.

REFERENCES

(1) R. Eisenmann and B.E. Kaminski, "Fracture control for composite structures," Engng. Fracture Mech. 4, 907-913 (1972).

(2) T.E. Hess, S.L. Huang and H. Robin, "Fracture control in composite materials using integral crack arresters," Proc. of AIAA/ASME/SAE 17th Structures, Structural Dynamics, and Material Conference, 52-60 (1976).

(3) J.G. Avery and T.R. Porter, "Damage tolerant structural concepts for fiber composites," Proc. Army Symp. on Solid Mechanics, AMMRC-MS-76-2 (1976).

(4) R.M. Verette and J.M. Labor, "Structural criteria for advanced composites," AFFDL-TR-142 (1976).

(5) C.C. Poe, Jr. and J.M. Kennedy, "An assessment of buffer-strips for improving damage tolerance of composite laminates," J. Comp. Materials, Suppl 14, 57-70 (1980).

(6) J.G. Goree and R.S. Gross, "Analysis of unidirectional composite containing broken fibers and matrix damage," Engng. Fracture Mech. 13, 563-578 (1979).

(7) L.R. Dharani, W.F. Jones and J.G. Goree, "Mathematical modeling of damage in unidirectional composites," Engng. Fracture Mech. 17(6), 555-573 (1983).

(8) A.K. Kaw, and J.G. Goree, "Shear-lag analysis of notched laminates with interlaminar debonding," Engng. Fracture Mech. 22(6), 1013-1029 (1985).

(9) L.R. Dharani and J.G. Goree, "Analysis of unidirectional symmetric buffer-strip laminate with damage," Engr. Fracture Mech. 20 (5/6),801-811 (1984).

(10) L.R. Dharani and J.G. Goree, "Residual strength of a unidirectional, symmetric buffer-strip laminate with fiber and matrix damage," Proc. Secfam XII, 541-546, (May, 1984).

(11) C. Zweben, "Fracture mechanics and composite materials: A critical analysis," ASTM, 65-97, (1973).

(12) P. Kuhn, "Stresses in aircraft and shell structures," McGraw Hill, New York, (1962).

(13) S.B. Batdorf, "Measurements of local stress distribution in damaged composites using an electric analog." Adv. in Aerospace Str. and Mats., 71-74, (1982).

(14) J.M. Hedgepeth, "Stress concentrations for filamentary structures," NASA TN D-882, (1961).